J. Ocean Univ. China (Oceanic and Coastal Sea Research)
https://doi.org/10.1007/s11802-019-3974-7
ISSN 1672-5182, 2019 18 (3): 654-662
http://www.ouc.edu.cn/xbywb/
E-mail:xbywb@ouc.edu.cn

Metabolomic Fingerprint of the Model Ciliate, *Tetrahymena thermophila* Determined by Untargeted Profiling Using Gas Chromatography-Mass Spectrometry

XU Jing[1), 2), #], BO Tao[2), #], SONG Weibo[1)], and WANG Wei[2), *]

1) *Institute of Evolution & Marine Biodiversity*, *Ocean University of China*, *Qingdao* 266003, *China*
2) *Key Laboratory of Chemical Biology and Molecular Engineering of Ministry of Education*, *Institute of Biotechnology*, *Shanxi University*, *Taiyuan* 030006, *China*

(Received August 1, 2018; revised September 26, 2018; accepted December 24, 2018)

Abstract The ciliate *Tetrahymena* is a valuable model organism in the studies of ecotoxicology. Changes in intracellular metabolism are caused by exogenous chemicals in the environment. Intracellular metabolite changes signify toxic effects and can be monitored by metabolomics analysis. In this work, a protocol for the GC-MS-based metabolomic analysis of *Tetrahymena* was established. Different extraction solvents showed divergent effects on the metabolomic analysis of *Tetrahymena thermophila*. The peak intensity of metabolites detected in the samples of extraction solvent Formula 1 (F1) was the strongest and stable, while 61 metabolites were identified. Formula 1 showed an excellent extraction performance for carbohydrates. In the samples of extraction solvent Formula 2 (F2), 66 metabolites were characterized, and fatty acid metabolites were extracted. Meanwhile, 57 and 58 metabolites were characterized in the extraction with Formula 3 (F3) and Formula 4 (F4), respectively. However, the peak intensity of the metabolites was low, and the metabolites were unstable. These results indicated that different extraction solvents substantially affected the detected coverage and peak intensity of intracellular metabolites. A total of 74 metabolites (19 amino acids, 11 organic acids, 2 inorganic acids, 11 fatty acids, 11 carbohydrates, 3 glycosides, 4 alcohols, 6 amines, and 7 other compounds) were identified in all experimental groups. Among these metabolites, amino acids, glycerol, myoinositol, and unsaturated fatty acids may become potential biomarkers of metabolite set enrichment analysis for detecting the ability of *T. thermophila* against environmental stresses.

Key words *Tetrahymena thermophila*; metabolomics; ecotoxicology; gas chromatography-mass spectrometry

1 Introduction

Metabolomics is an effective technique to determine the metabolic response of organisms to environmental stimuli (Bundy *et al*., 2009). The technology has been applied recently in ecotoxicology since it can evaluate the toxicity of pollutants by displaying detailed information on the changes of endogenous small molecule metabolites in organisms under different stresses (Gillis *et al*., 2017). Remarkable metabolic changes in organisms can be induced by environmental toxicants, and these changes precede traditional ecotoxicology endpoints such as death and decreased reproductive capacity (Heijne *et al*., 2005; Viant *et al*., 2006; Ekman *et al*., 2007; Zhao *et al*., 2018). Therefore, metabolomics can provide valid information for evaluating the mode of action of a compound at sublethal concentrations and complement traditional ecotoxicology endpoints (Aliferis and Jabaji, 2011).

The ciliate *Tetrahymena* is a free-living ciliate group that is ubiquitous in water ecosystems worldwide, and its structural and functional complexity is similar to that of metazoan cells (Collins and Gorovsky, 2005). *Tetrahymena thermophila* display nuclear dimorphism containning germline micronucleus (MIC) and somatic macronucleus (MAC) (Gao *et al*., 2013; Xiong *et al*., 2016). The MIC is transcriptionally silent during the vegetative growth and is the storage of genetic information for the sexual progeny. The MAC is transcriptionally active in the vegetative cells and directly determines the phenotype of cell (Wang *et al*., 2017a; Wang *et al*., 2017b; Zhang *et al*., 2018). *T. thermophila* has been used as model organism in the studies of genetics, cell biology, and toxicology (Xu *et al*., 2015; Chen *et al*., 2016b; Zhao *et al*., 2017; Wang *et al*., 2017c). It is highly sensitive to toxicants. In specific, toxicants can suppress the growth of *T. thermophila* and inhibit cell mobility. The close relationship exists between individual behavior and environmental pollution (Bonnet *et al*., 2008; Bricheux *et al*., 2013). Therefore, *T. thermophila* is an ideal early warning indicator for assessing water ecosystems (Sauvant *et al*., 1999; Luo *et al*., 2015). Ecotoxicological studies with *Tetrahymena* as a test organism elucidated the mechanism

# These authors contributed equally.
∗ Corresponding author. E-mail: gene@sxu.edu.cn

of toxicants' functions mainly by comet assay, microscopic observation, fluorescent staining, and transcriptomics analysis (Feng *et al*., 2014; Li *et al*., 2015; Luo *et al*., 2015). However, the effect of toxicants on the intracellular metabolism of *Tetrahymena* remains unclear.

In the present study, different water-methanol-chloroform mixtures were used as extraction solvents for the global metabolite profiling of *T. thermophila*. We compared the extraction effects of different extracts on the intracellular metabolites of *T. thermophila* and then determined the best extract formula. Meanwhile, cell harvest, extraction and analytical protocols for the gas chromatography-mass spectrometry (GC-MS)-based metabolomic analysis of *Tetrahymena* were established, and a new perspective in ecotoxicology using *Tetrahymena* was provided.

2 Materials and Methods

2.1 *Tetrahymena* Strain and Culture Conditions

CU428 (mpr1-1/mpr1-1 [VII, mp-s]) was initially obtained from Dr. Peter J. Bruns (Cornell University, Ithaca, NY, USA) and is available through the National *Tetrahymena* Stock Center (http://tetrahymena.vet.cornell.edu/index.html). Cells were cultured in SPP medium (1% peptone, 0.2% glucose, 0.1% yeast extract, 0.003% EDTA iron salt (pH 7.4)) at 30℃ for 12 h, and the initial cell density was adjusted to (2.0–3.0)×10^4 cells mL^{-1} (Wang *et al*., 2017).

2.2 Metabolite Extraction and Derivatization

The samples were divided into four groups with different extraction solvents including Formula 1 (F1): ultrapure water-methanol (5:5); Formula 2 (F2): ultrapure water-methanol-chloroform (5:12.5:5); Formula 3 (F3): ultrapure water-methanol-chloroform (5:16:4); Formula 4 (F4): ultrapure water-methanol-chloroform (5:24:6). Six independent metabolite extractions were performed for each group. *T. thermophila* at exponential phase was harvested by centrifugation (3000 r min^{-1} for 5 min) and washed twice with 10 mmol L^{-1} TBS buffer (pH 7.4). Then, metabolism quenching was accomplished by liquid nitrogen, and the cells were ground into fine powder in liquid nitrogen. Ground cells (50 mg) were suspended in 1 mL of extraction buffer and then mixed thoroughly. For metabolite extraction, five cycles of snap-freezing with liquid nitrogen for 2 min in every cycle were performed with the mixture. After centrifugation (5000 r min^{-1} for 3 min at 4℃), the supernatant was collected, and 100 μL metabolic extracts containing 20 μL of internal standard solution (succinic-*d4* acid, 1.6 mg mL^{-1}, Sigma) were vacuum-dried and stored at −80℃ for further derivatization. A two-stage chemical derivatization was performed before GC-MS analysis as described previously (Bo *et al*., 2014; Chen *et al*., 2018).

2.3 GC-MS Analysis

GC-MS analysis was performed by an Agilent 7890A gas chromatograph equipped with a 5795C mass spectrometry detector with electron-impact ionization source in the selective ion monitoring mode. An HP-5-fused silica capillary column (30 m length × 0.25 mm diameter × 0.25 μm film thickness) was used for separating each compound. High-purity helium was set at a constant flow of 1 mL min^{-1}. The electron impact ionization (70 eV) was set at a full scan mode (m/z 50–800). Samples (1 μL) were injected with a split ratio of 1:10. The temperatures for injection, ion source, and ion source surface were set to be 280℃, 250℃, and 280℃, respectively. The GC oven temperature was maintained at 70℃ for 2 min, followed by a temperature ramp at 5℃ min^{-1} until 290℃, which was held for 3 min. MSD Oroductivity ChemStation software (version E.0201.1177, Agilent Technologies) was used to acquire mass spectrometric data.

2.4 Data Mining

Principal component analysis (PCA) and hierarchical clustering (HCA) were performed as previously described (Bo *et al*., 2014). The 'Range' and 'Formula' of 'Normalization' in step 2 (Data Transformation) for HCA in HCE 3.5 software checked the 'column-by-column' and $\frac{x-m}{\sigma}$, respectively. In addition, metabolome coverage among the four extracts and different species was compared by Venn diagrams (Oliveros, 2015). Matabolite set enrichment analysis (MSEA) was performed using metaboanalyst (Xia *et al*., 2009).

3 Results

3.1 Metabolic Extraction Assessment

The total ion chromatogram for the intracellular metabolites of *T. thermophila* obtained using the four extraction solvents is shown in Fig.1. The four metabolite profiles were remarkably different based on the peak intensity in the chromatogram. F1 extracts presented the greatest overall intensity (Fig.1). Through analysis and comparison of the data, a total of 126 metabolite signals were detected, and 74 metabolites were characterized in the four experimental groups. 61, 66, 57, and 58 metabolites were identified in the groups of F1, F2, F3, and F4, respectively (Table 1). In addition, amino acids, carbohydrates, glycosides, organic acids, fatty acids, inorganic acids, amines, alcohols, and intermediate metabolites were identified in the metabolites.

A total of 47 metabolites were common in the different groups, accounting for 62.7% of the total metabolite species (Fig.2A). Compared with those of the other three groups, the metabolic coverage of F1 was divergent (Fig.2A and Table 1). Seven metabolites, namely, D-xylose, 2,3,4,5-tetrahydroxypentanoic acid-1, 4-lactone, β-D-manno pyranoside, D-(-)-fructofuranose, D-glucopyranoside, myristic acid, and inositol, were uniquely found in the samples of F1. A total of 54 types of metabolites were shared between F1 and F2 (Fig.2B). Meanwhile, 12 metabolites including citrulline, tetradecanoic acid, palmitelaidic acid,

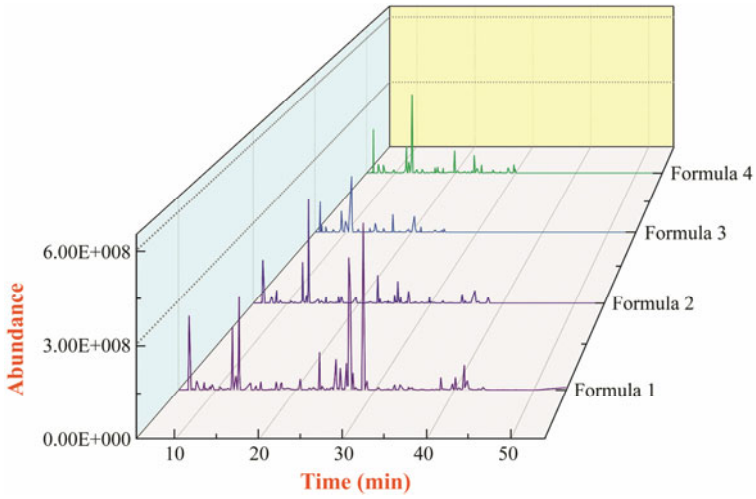

Fig.1 The typical GC-MS total ion chromatograms of the intracellular small molecule metabolites of *T. thermophila.* The metabolites of the cells were extracted with different extraction solvent. Formula 1: ultrapure water-methanol; Formula 2: ultrapure water-methanol-chloroform; Formula 3: ultrapure water-methanol-chloroform; Formula 4: ultrapure water-methanol-chloroform.

Table 1 Comparison of metabolites in different extraction solvents

Metabolites	Extraction solvents				Metabolites	Extraction solvents			
	F1	F2	F3	F4		F1	F2	F3	F4
L-Valine	●	●	●	●	Octadecanoic acid	–	●	–	–
l-Alanine	●	●	●	●	9,12-Octadecadienoic acid	–	●	●	●
Glycine	●	●	●	●	9,12,15-Octadecatrienoic acid	–	●	–	–
l-Leucine	●	●	●	●	Oleic acid	–	●	●	●
l-Proline	●	●	●	●	Hexadecanoic acid	–	●	–	–
l-Isoleucine	●	●	●	●	Myristic acid	●	–	–	–
Serine	●	●	●	●	D-Xylose	●	–	–	–
l-Methionine	●	●	●	●	Arabinose	●	●	●	●
l-Aspartic acid	●	●	●	●	Arabinofuranose	●	●	●	●
L-Cysteine	●	●	●	●	D-(-)-Fructofuranose	●	–	–	–
L-Asparagine	●	●	●	●	D-(-)-Ribofuranose	●	●	–	–
Ornithine	●	●	●	●	d-Galactose	●	●	●	●
Glutamic acid	●	●	●	●	D-(+)-Talose	●	●	●	●
l-Glutamine	●	●	●	●	D-Lactose	●	●	●	●
L-Lysine	●	●	●	●	D-(+)-Cellobiose	●	●	●	●
L-threonine	●	●	●	●	Maltose	●	●	●	●
L-Tyrosine	●	●	●	●	β-D-Glucopyranose	●	●	●	●
Citrulline	–	●	●	–	Glycoside	●	●	●	●
Glycyl-l-glutamic acid	●	●	–	–	D-glucopyranoside	●	–	–	–
Propanoic acid	●	●	●	●	β-D-Mannopyranoside	●	–	–	–
Ethanedioic acid	●	●	●	●	Glycerol	●	●	●	●
Butanoic acid	●	●	●	–	Myo-Inositol	●	●	●	●
Butanedioic acid	●	●	●	●	Inositol	●	–	–	–
2-Butenedioic acid	●	●	●	●	1-O-hexadecylglycerol	–	●	●	●
Aminomalonic acid	●	●	–	–	Myo-Inositol-phosphate	●	●	–	–
Pentanedioic acid	●	●	●	●	d-Fructose-6-phosphate	●	●	●	●
Tetrahydroxypentanoic acid	●	–	–	–	d-Glucose-6-phosphate	●	●	●	●
Phosphonic acid	●	●	●	●	Pyrimidine	●	●	●	●
3-Pyridinecarboxylic acid	–	–	–	●	9H-Purine	●	●	●	●
Cyclohexaneacetic acid	–	–	–	●	Guanosine	●	●	–	–
Phosphoric acid	●	●	●	●	hydroxylamine	●	●	●	●
Acetic acid	●	●	–	●	Cadaverine	●	●	●	●
Tetradecanoic acid	–	●	●	●	aminomethane	●	●	●	●
Dodecanoic acid	●	●	●	●	acetamide	●	●	●	●
Palmitelaidic acid	–	●	●	●	1,4-Butanediamine	●	●	●	●
Heptadecanoic acid	–	●	●	●	Spermine	–	●	●	●
Linolenic acid	–	●	●	●	Inosine	●	●	●	●

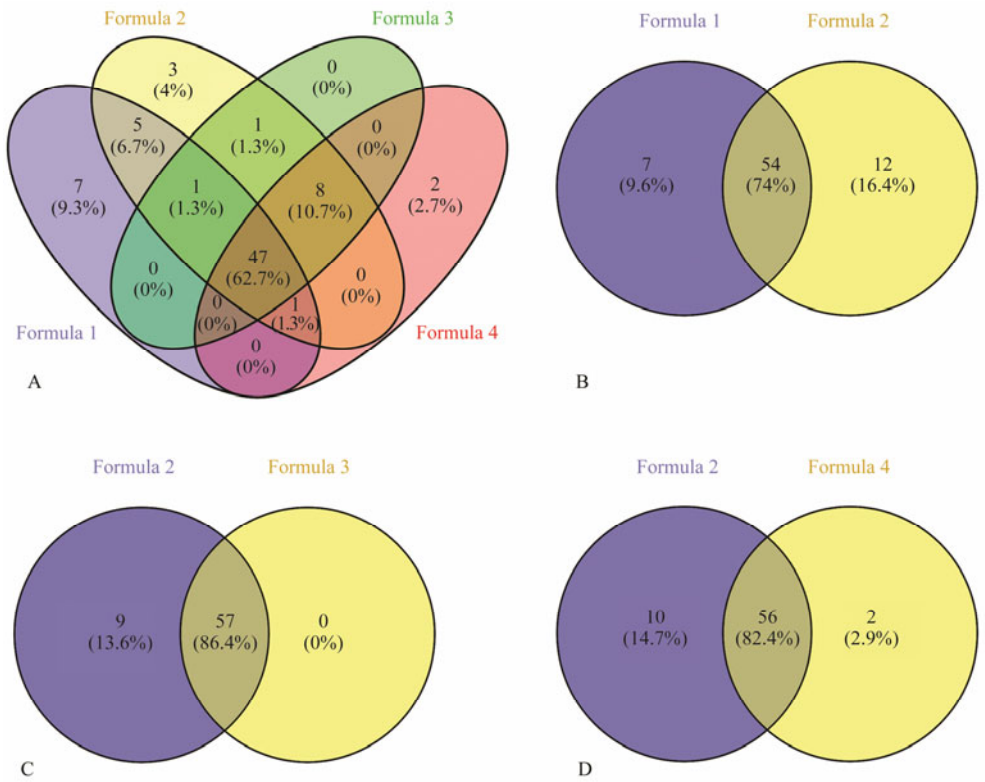

Fig.2 Venn diagrams of intracellular small molecule metabolites of *T. thermophila.* The overlap of the intracellular small molecule metabolites extracted with different extraction solvents from *T. thermophila.* (A) Comparison of the metabolic coverage among Formula 1, Formula 2, Formula 3, and Formula 4; (B) Comparison of the metabolic coverage between Formula 1 and Formula 2; (C) Comparison of the metabolic coverage between Formula 2 and Formula 3; (D) Comparison of the metabolic coverage between Formula 2 and Formula 4. The experiments were conducted in six replicates, and the metabolites that appeared more than four times stably in six replicates were used for analysis.

heptadecanoic acid, linolenic acid, 9,12-octadecadienoic acid, oleic acid, spermine, 1-O-hexadecylglycerol, octadecatrienoic acid, hexadecanoic acid, and octadecanoic acid were distinctively found in F2. Chloroform was contained in the three extraction solvents of F2, F3, and F4. Among the four groups, F2 showed the highest overall metabolome coverage in terms of the number of identified metabolites, and it can cover all metabolites in F3 and all metabolites, except 3-pyridinecarboxylic acid and cyclohexaneacetic acid in F4 (Figs.2C and 2D).

3.2 Metabolic Profiles of *T. thermophila*

A total of 74 intracellular small molecule metabolites in the four extracts were analyzed by hierarchical clustering analysis (HCA), an unsupervised pattern recognition method. Fig.3 visualizes the results of HCA in the heat map, and distinct clustering was observed among the four groups. Each solvent can extract small molecule metabolites in a different way. F1 was obvious different with the other three groups of extraction solvents containing chloroform. In the heat map, the color represents the normalized peak area (the highest values shown in red and the lowest in green). The normalized peak area for most of the metabolites detected in F1 is red, indicating that the concentration of these metabolites is the highest in F1 among the four groups. However, the concentration of fatty acid metabolites in F2, F3, and F4 were remarkably higher than those in F1.

We performed PCA to further verify the differences and identify the metabolites that were mainly responsible for the discrimination among different experimental groups. As shown in the PCA score plot (Fig.4A), the four experimental groups exhibited apparent discrepancies, suggesting that different formulations of extraction solvent could affect metabolomics analysis of *Tetrahymena*. PCA also further verified the predictive accuracy of HCA. In addition, F1 was markedly different with the other three groups, indicating great differences in the concentration and coverage of metabolites in F1 group compared with the other groups. As shown in the loading plot of PCA (Fig.4B), leucine, glycoside, phosphoric acid, galactose, inosine, lactose, and cellobiose were the most influential metabolites responsible for the difference between different groups. Among the solvents, F1 exerted the most favorable extraction effect on these metabolites (Fig.5). In conclusion, the strongest peak intensity of the metabolites was detected in F1, followed by that in F2. Furthermore, F1 exerted a strong effect on the extraction of carbohydrates, and the extraction effect of F2 on fatty acid was the best among the groups. On the other hand, the solid circles representing the six parallel samples in the same experimental group were close to each other, and some even overlapped based on the score plot of PCA. The results also indicated that the technology used in this study had excellent stability and repeatability.

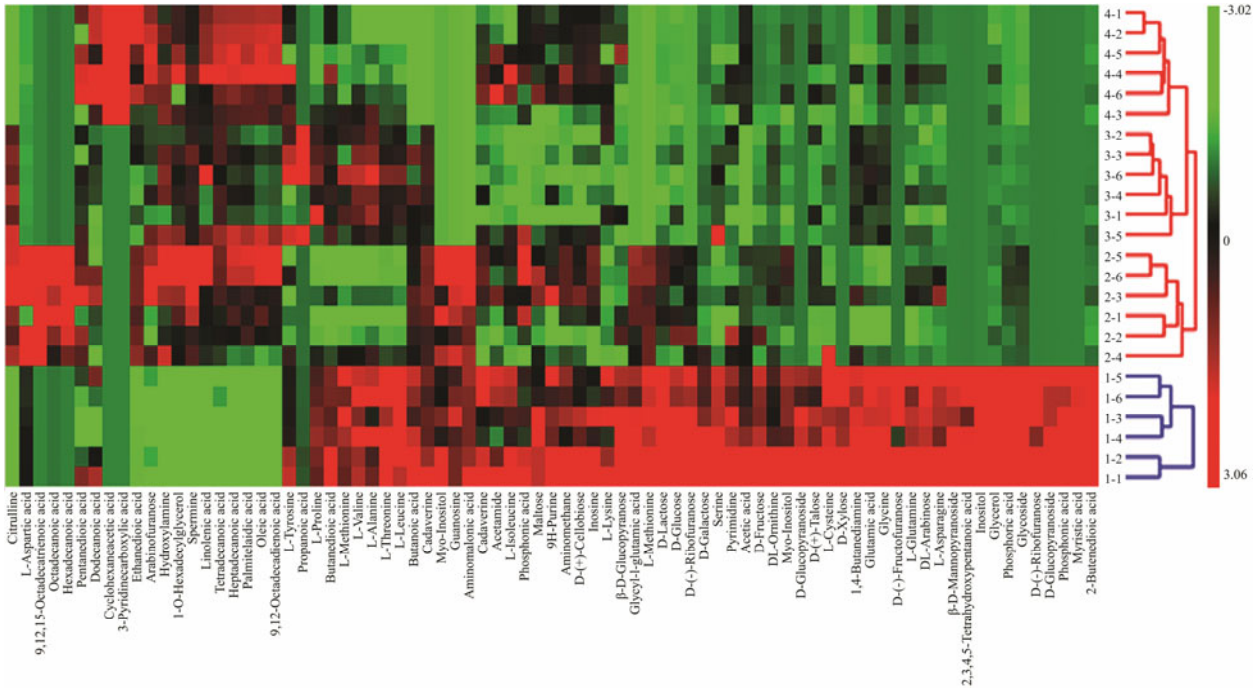

Fig.3 Hierarchical cluster analysis of the identified metabolites in *T. thermophila.* The samples were extracted with different extraction solvents. Heat map represents unsupervised hierarchical clustering of groups. The row displays metabolite and the column represents the samples. The colors from green to red indicate the increasing expression of metabolites. The brightness of each color corresponded to the magnitude of the difference when compared with the average value. The experiments were conducted with six replicates.

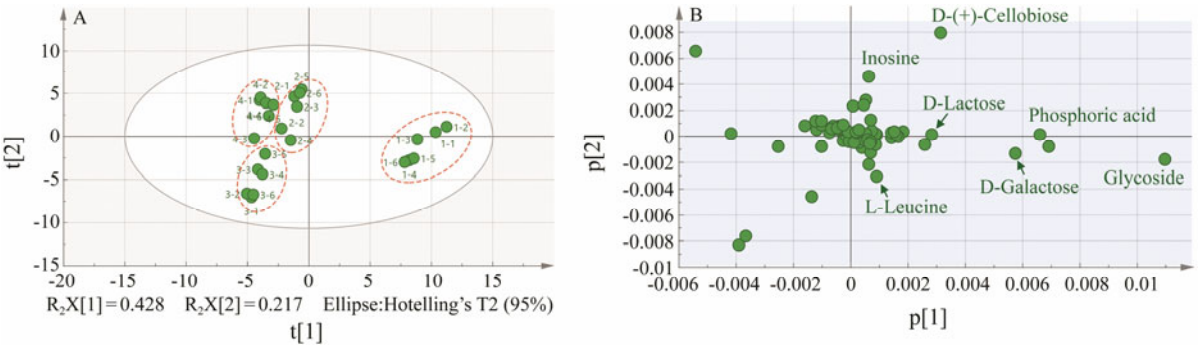

Fig.4 The principal component analysis of intracellular small molecule metabolites of *T. thermophila.* (A) PC 1, 42.8% of total variance; PC 2, 21.7% of total variance. In the scores plot, the confidence interval is defined by Hotelling's T2 ellipse (95% confidence interval), and observations outside the confidence ellipse are considered outliers; (B) Loading plot of samples from Formula 1, Formula 2, Formula 3 and Formula 4. The experiments were conducted with six replicates.

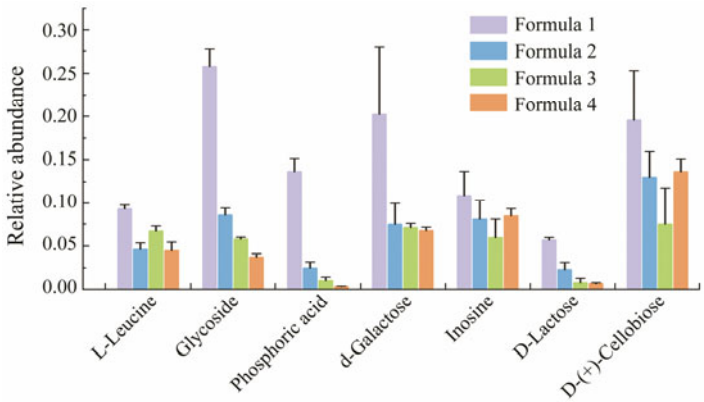

Fig.5 Comparison of the relative peak intensities of seven small molecular metabolites. The metabolites of the cells were extracted with different extraction solvents. Formula 1: ultrapure water-methanol; Formula 2: ultrapure water-methanol-chloroform; Formula 3: ultrapure water-methanol-chloroform; Formula 4: ultrapure water-methanol-chloroform. Each value is the mean of six replicates ± standard deviation (SD).

3.3 Metabolite Set Enrichment Analysis (MSEA) of *T. thermophila*

The identified metabolites were submitted to enrichment analysis using MSEA by over representation analysis to determine the more represented metabolic pathway in a defined set of metabolites. As shown in Fig.6, the metabolic pathway involved in protein synthesis contained the greatest number of metabolites detected (14 out of 19 metabolites in the pathway). Moreover, 'ammonia recycling', 'urea cycle', 'methionine metabolism', 'galactose metabolism', 'glutathione metabolism', 'arginine and proline metabolism', and 'aspartate metabolism' were the metabolic pathways in which a high number of the metabolites were related.

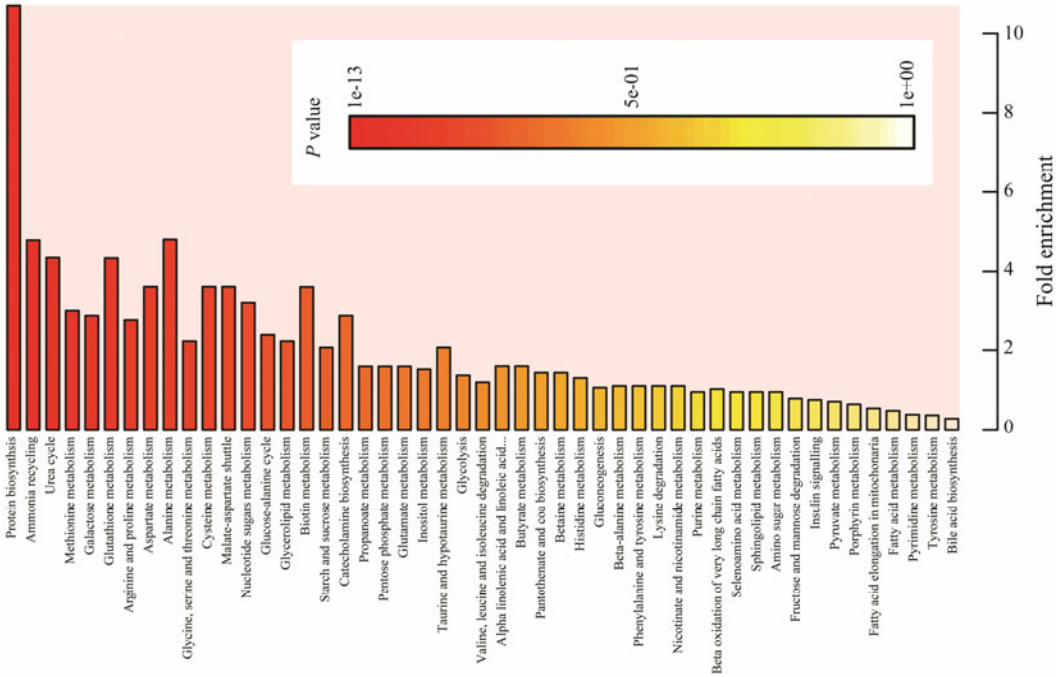

Fig.6 Summary plot for metabolite set enrichment analysis of *T. thermophila.* MSEA was implemented using the hypergeometric test to evaluate whether a particular metabolite set is represented more than expected by chance within the given compound list. One-tailed p values are provided after adjusting for multiple testing.

4 Discussion

4.1 Comparison of Extraction Performance of Different Extraction Solvents

The most common solvents for metabolite extraction include an organic solvent or a mixture of organic solvents such as methanol, water-methanol (1:3) or water-methanol-chloroform (10:27:3) (García-Cañaveras *et al*., 2016). Intracellular metabolites have been extracted from yeast, bacteria, or mammalian cells by a water-methanol-chloroform mixture (Cao *et al*., 2011). In *Tetrahymena*, on the basis of the TIC and the heat map of HCA (Figs.1 and 3) of the four groups, the strongest peak intensity of the metabolites was detected in F1 possibly due to the higher proportion of water in F1 than the other extraction solvents. The result is consistent with the findings of Ibáñez *et al*. (2017), who compared the effects of acetonitrile, acetonitrile-isopropanol-water (3:3:1), water, and 5% formic acid solution on the extraction of intracellular metabolites of human colon cancer cells. They found that the detected metabolite signal is stronger in the two aqueous-based extractions, namely, water and acidified water (5% formic acid solution) (Ibáñez *et al*., 2017). In the present study, we found a difference in the coverage of metabolites from the different solvents mainly because of the polarity of the solvent. As a typical polar solvent consisting of water and methanol, F1 can extract more polar metabolites such as carbohydrates and glycosides than the other solvents. By contrast, more fatty acid metabolites were extracted by F2, F3, and F4 due to their chloroform content. Chloroform is a nonpolar solvent that is often used to extract fatty acids (Evans *et al*., 1998).

In order to evaluate the validity of the protocol for metabolomic fingerprint analysis of *Tetrahymena*, the identified metabolites of *Tetrahymena* were compared with *Saccaromyces cerevisiae*, Zingiberaceae plants, and human colon cancer cells (Bo *et al*., 2014; Barbosa *et al*., 2017; Ibáñez *et al*., 2017). There were 74, 71, 87 and 150 metabolites identified from the above four species respectively, and 12 common metabolites were found, including 11 amino acids and myoinositol. In particular, 24 types of metabolites existed only in *Tetrahymena* cells, accounting for 9.2% of the total metabolites (Fig.7A), and these metabolites were mainly involved in organic acids and fatty acid. Comparison with *S. cerevisiae*, Zingiberaceae plants, and human colon cancer cells revealed that 38, 56, and 44 metabolites were unique to *Tetrahymena*, respectively (Figs.7B, 7C, and 7D). Compared with other studies, the metabolites of *Tetrahymena* were identified, including

common amino acids and carbohydrates, while metabolites unique to *Tetrahymena* were also identified. The results indicated that the protocol of metabolomic fingerprint analysis of *Tetrahymena* established in this study was effective. But remarkable differences in the number of metabolites identified by GC-MS were observed in the different samples. One of the main reasons for the differences may be due to the difference of species being analyzed. For example, in the same case of using methanol as the main component of the extraction solvent and analyzing with GC-Q MS, 79 intracellular metabolites in *Gluconacetobacter xylinus* were detected (Liu *et al*., 2015); 76 and 64 metabolites were identified respectively in the leaves and rhizomes of selected Zingiberaceae plants (Barbosa *et al*., 2017); 38 metabolites were qualitatively analyzed in human plasma (Zhou *et al*., 2016). The differences are caused not only by different types of samples, but also by the different GC-MS platform. For instance, the metabolomic fingerprint of *S. cerevisiae* was analyzed with the same extraction method, and 72 metabolites were identified using GC-Q MS in *S. cerevisiae* (Bo *et al*., 2014), while the number could be increased to 89 by using GC-TOF MS (Ding *et al*., 2011). Compared with GC-Q MS, the type of compound that can be detected is increased by GC-TOF MS due to its higher resolution and sensitivity, as well as the capability to detect high-molecular-weight compounds. Thus, solvents F1 and F2 were favorable in extracting intracellular metabolites of *T. thermophila* compared with these metabolomics study on different species based on GC-MS.

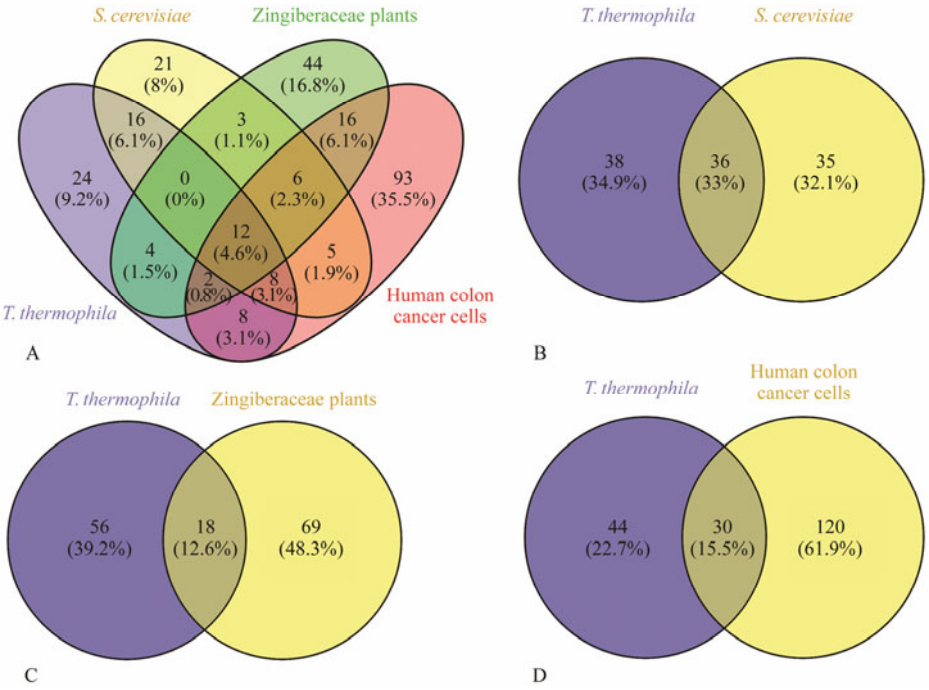

Fig.7 Venn diagrams of overlap of the intracellular small molecule metabolites from different species. The metabolites were compared among *Tetrahymena thermophila*, *Saccaromyces cerevisiae*, Zingiberaceae plants, and human colon cancer cells. A) Comparison of the metabolic coverage between *Tetrahymena*, *S. cerevisiae*, Zingiberaceae plants, and human colon cancer cells; (B) comparison of the metabolic coverage between *Tetrahymena* and *S. cerevisiae*; (C) comparison of the metabolic coverage between *Tetrahymena* and Zingiberaceae plants; (D) comparison of the metabolic coverage between *Tetrahymena* and human colon cancer cells.

4.2 Analysis of Potential Biomarkers of *T. thermophila*

As shown in Fig.6, the protein biosynthesis pathway was the metabolic pathway that contained a high number of metabolites, including glutamate, tyrosine, alanine, proline, threonine, asparagine, isoleucine, lysine, aspartic acid, cysteine, glutamine, leucine, methionine and valine. Amino acids are extremely important for protein synthesis and energy production. The concentrations of valine, leucine and isoleucine (branched chain amino acid), and phenylalanine, tyrosine and tryptophan (aromatic amino acids) plummeted remarkably in the earthworms treated by Pb. This was because that a burst of reactive oxygen species (ROS) induced by Pb could directly damage the structure of the proteins and even lead to disintegration. The decrease in the concentrations of amino acids proposed an increase in the synthesis of proteins for compensation (Chen *et al*., 2016a). Amino acids are important primary metabolites as well as the protective substances and biomarkers of cells responding to multiple external stresses (Jozefczuk *et al*., 2010; Chen *et al*., 2016a). For instance, aspartic acid is the biomarker and the only down-regulated metabolite of *Diporeia* responding to the stress of atrazine (Ralston-Hooper *et al*., 2008). Thus, amino acids may serve as potential biomarkers of *Tetrahymena* against environmental stresses.

Heavy metals can induce oxidative stress characterized by excessive ROS generation. ROS injures an organism by acting on biological macromolecules that cause protein oxidation, lipid peroxidation, and DNA damage. A primary

defense against oxidative damage is the glutathione redox system, which is important for maintaining cellular redox balance (Chen *et al*., 2016a). In the present study, the identified metabolites involved in the glutathione metabolic pathway included cysteine, glutamic acid, and glycine. Therefore, these three amino acids could serve as biomarkers of *T. thermophila* in response to oxidative stress. Glycerol, myoinositol, and unsaturated fatty acids, which can protect the cells from external stress, may also serve as biomarkers for *T. thermophila* to cope with environmental stress.

5 Conclusions

The coverage and signal intensity of intracellular metabolites were affected by different extraction solvents. Solvents F1 and F2 showed higher coverage and signal intensity of metabolites. Carbohydrates, glycoside and some amino acids could be extracted more efficiently with F1, while F2 was more effective in extracting fatty acids than the other solvents. Among these identified metabolites, amino acids, glycerol, myoinositol, and unsaturated fatty acids may become potential biomarkers for detecting the ability of *T. thermophila* against environmental stress. To the best of our knowledge, this study is the first one to analyze the cellular metabolome of *T. thermophila*. Meanwhile, a protocol for the GC-MS-based metabolomic analysis of *T. thermophila* was established, and a new observation endpoint was added for ecotoxicological evaluation using *Tetrahymena*.

Acknowledgements

This study was supported by the National Natural Science Foundation of China (Nos. 31572253, 31601857, 31702009), the Science Foundation for Youths of Shanxi Province (No. 201801D221241), and the Postdoctoral Science Foundation of China (No. 2014M551961).

References

Aliferis, K. A., and Jabaji, S., 2011. Metabolomics–A robust bioanalytical approach for the discovery of the modes-of-action of pesticides: A review. *Pesticide Biochemistry and Physiology*, **100**: 105-117.

Barbosa, G. B., Jayasinghe, N. S., Natera, S. H., Inutan, E. D., Peteros, N. P., and Roessner, U., 2017. From common to rare zingiberaceae plants□A metabolomics study using GC-MS. *Phytochemistry*, **140**: 141-150.

Bo, T., Liu, M., Zhong, C., Zhang, Q., Su, Q., Tan, Z., Han, P., and Jia, S., 2014. Metabolomic analysis of antimicrobial mechanisms of ε-poly-l-lysine on *Saccharomyces cerevisiae*. *Journal of Agricultural and Food Chemistry*, **62**: 4454-4465.

Bonnet, J. L., Bonnemoy, F., Dusser, M., and Bohatier, J., 2008. Toxicity assessment of the herbicides sulcotrione and mesotrione toward two reference environmental microorganisms: *Tetrahymena pyriformis* and *Vibrio fischeri*. *Archives of Environmental Contamination and Toxicology*, **55**: 576-583.

Bricheux, G., Bonnet, J. L., Bohatier, J., Morel, J. P., and Morel-Desrosiers, N., 2013. Microcalorimetry: A powerful and original tool for tracking the toxicity of a xenobiotic on *Tetrahymena pyriformis*. *Ecotoxicology and Environmental Safety*, **98**: 88-94.

Bundy, J. G., Davey, M. P., and Viant, M. R., 2009. Environ mental metabolomics: A critical review and future perspectives. *Metabolomics*, **5**: 3.

Cao, B., Aa, J., Wang, G., Wu, X., Liu, L., Li, M., Shi, J., Wang, X., Zhao, C., and Zheng, T., 2011. GC-TOFMS analysis of metabolites in adherent MDCK cells and a novel strategy for identifying intracellular metabolic markers for use as cell amount indicators in data normalization. *Analytical and Bioanalytical Chemistry*, **400**: 2983-2993.

Chen, T., Liu, Y., Li, M.-H., Xu, H., Sheng, J., Zhang, L., and Wang, J., 2016a. Integrated 1H NMR-based metabolomics analysis of earthworm responses to sub-lethal Pb exposure. *Environmental Chemistry*, **13**: 792-803.

Chen, X., Gao, S., Liu, Y., Wang, Y., Wang, Y., and Song, W., 2016b. Enzymatic and chemical mapping of nucleosome distribution in purified micro- and macronuclei of the ciliated model organism, *Tetrahymena thermophila*. *Science China Life Science*, **59**: 909-19.

Chen, X., Wang, Y. R., Sheng, Y. L., Warren, A., and Gao, S., 2018. GPSit: An automated method for evolutionary analysis of nonculturable ciliated microeukaryotes. *Molecular Ecology Resources*, **18**: 700-713.

Collins, K., and Gorovsky, M. A., 2005. *Tetrahymena thermophila*. *Current Biology*, **15**: 317-318.

Ding, M., Wang, X., Yang, Y., and Yuan, Y., 2011. Metabolomic study of interactive effects of phenol, furfural, and acetic acid on *Saccharomyces cerevisiae*. *Omics*, **15**: 647-653.

Ekman, D., Teng, Q., Jensen, K., Martinovic, D., Villeneuve, D., Ankley, G., and Collette, T., 2007. NMR analysis of male fathead minnow urinary metabolites: A potential approach for studying impacts of chemical exposures. *Aquatic Toxicology*, **85**: 104-112.

Evans, R. I., McClure, P. J., Gould, G. W., and Russell, N. J., 1998. The effect of growth temperature on the phospholipid and fatty acyl compositions of non-proteolytic *Clostridium botulinum*. *International Journal of Food Microbiology*, **40**: 159-167.

Feng, L., Fu, C., Yuan, D., and Miao, W., 2014. A P450 gene associated with robust resistance to DDT in ciliated protozoan, *Tetrahymena thermophila* by efficient degradation. *Aquatic Toxicology*, **149**: 126-132.

Gao, S., Xiong, J., Zhang, C., Berquist, B. R., Yang, R., Zhao, M., Molascon, A. J., Kwiatkowski, S. Y., Yuan, D., Qin, Z., Wen, J., Kapler, G. M., Andrews, P. C., Miao, W., and Liu, Y., 2013. Impaired replication elongation in *Tetrahymena* mutants deficient in histone H3 Lys 27 monomethylation. *Genes & Development*, **27**: 1662-79.

García-Cañaveras, J. C., López, S., Castell, J. V., Donato, M. T., and Lahoz, A., 2016. Extending metabolome coverage for untargeted metabolite profiling of adherent cultured hepatic cells. *Analytical and Bioanalytical Chemistry*, **408**: 1217-1230.

Gillis, J. D., Price, G. W., and Prasher, S., 2017. Lethal and sublethal effects of triclosan toxicity to the earthworm *Eisenia fetida* assessed through GC-MS metabolomics. *Journal of Hazardous Materials*, **323**: 203-211.

Heijne, W. H., Kienhuis, A. S., Van Ommen, B., Stierum, R. H., and Groten, J. P., 2005. Systems toxicology: Applications of toxicogenomics, transcriptomics, proteomics and metabolomics in toxicology. *Expert Review of Proteomics*, **2**: 767-780.

Ibáñez, C., Simó, C., Palazoglu, M., and Cifuentes, A., 2017.

GC-MS based metabolomics of colon cancer cells using different extraction solvents. *Analytica Chimica Acta*, **986**: 48-56.

Jozefczuk, S., Klie, S., Catchpole, G., Szymanski, J., Cuadros-Inostroza, A., Steinhauser, D., Selbig, J., and Willmitzer, L., 2010. Metabolomic and transcriptomic stress response of *Escherichia coli*. *Molecular Systems Biology*, **6**: 364.

Li, W., Li, H., Zhang, J., and Tian, X., 2015. Effect of melamine toxicity on *Tetrahymena thermophila* proliferation and metallothionein expression. *Food and Chemical Toxicology*, **80**: 1-6.

Liu, M., Zhong, C., Wu, X., Wei, Y., Bo, T., Han, P., and Jia, S., 2015. Metabolomic profiling coupled with metabolic network reveals differences in *Gluconacetobacter xylinus* from static and agitated cultures. *Biochemical Engineering Journal*, **101**: 85-98.

Luo, H., Li, X., Fang, T., Liu, P., Zhang, C., Xie, H., and Sun, E., 2015. The toxicity of binary mixture of Cu (II) ion and phenols on *Tetrahymena thermophila*. *Ecotoxicology and Environmental Safety*, **113**: 412-417.

Oliveros, J. C., 2015. VENNY. An interactive tool for comparing lists with Venn diagrams. http://bioinfogp.cnb.csic.es/tools/venny/index.html.

Ralston-Hooper, K., Hopf, A., Oh, C., Zhang, X., Adamec, J., and Sepúlveda, M. S., 2008. Development of GCxGC/TOF-MS metabolomics for use in ecotoxicological studies with invertebrates. *Aquatic Toxicology*, **88**: 48-52.

Sauvant, N., Pepin, D., and Piccinni, E., 1999. *Tetrahymena pyriformis*: A tool for toxicological studies. *Chemosphere*, **38**: 1631-1669.

Viant, M. R., Pincetich, C. A., and Tjeerdema, R. S., 2006. Metabolic effects of dinoseb, diazinon and esfenvalerate in eyed eggs and alevins of *Chinook salmon (Oncorhynchus tshawytscha*) determined by 1 H NMR metabolomics. *Aquatic Toxicology*, **77**: 359-371.

Wang, C. D., Zhang, T. T., Wang, Y. R., Katz, L. A., Gao, F., and Song, W., 2017. Disentangling sources of variation in SSU rDNA sequences from single cell analyses of ciliates: Impacts of copy number variation and experimental errors. *Proceedings of the Royal Society B: Biological Sciences*, **284**: 2017 0425.

Wang, Y. Y., Chen, X., Sheng, Y., Liu, Y., and Gao, S., 2017a. N6-adenine DNA methylation is associated with the linker DNA of H2A.Z-containing well-positioned nucleosomes in Pol II-transcribed genes in *Tetrahymena*. *Nucleic Acids Research*, **45**: 11594-11606.

Wang, Y. Y., Sheng, Y., Liu, Y., Pan, B., Huang, J., Warren, A., and Gao, S., 2017b. N(6)-methyladenine DNA modification in the unicellular eukaryotic organism *Tetrahymena thermophila*. *European Journal of Protistology*, **58**: 94-102.

Wang, Y. R., Wang, Y., Sheng, Y., Huang, J., Chen, X., Al-Rasheid, K. A. S., and Gao, S., 2017c. A comparative study of genome organization and epigenetic mechanisms in model ciliates, with an emphasis on *Tetrahymena*, *Paramecium* and *Oxytricha*. *European Journal of Protistology*, **61**: 376-387.

Xia, J., Psychogios, N., Young, N., and Wishart, D. S., 2009. MetaboAnalyst: A web server for metabolomic data analysis and interpretation. *Nucleic Acids Research*, **37**: 652-660.

Xiong, J., Gao, S., Dui, W., Yang, W., Chen, X., Taverna, S. D., Pearlman, R. E., Ashlock, W., Miao, W., and Liu, Y., 2016. Dissecting relative contributions of cis- and trans-determinants to nucleosome distribution by comparing *Tetrahymena* macronuclear and micronuclear chromatin. *Nucleic Acids Research*, **44**: 10091-10105.

Xu, J., Yuan, Y., Liang, A., and Wang, W., 2015. Chromodomain protein Tcd1 is required for macronuclear genome rearrangement and repair in *Tetrahymena*. *Scientific Reports*, **5**: 10243.

Zhang, T. T., Wang, C. D., Katz, L. A., and Gao, F., 2018. A paradox: Rapid evolution rates of germline-limited sequences are associated with conserved patterns of rearrangements in cryptic species of *Chilodonella uncinata* (Protist, Ciliophora). *Science China Life Science*, **61**: 1071-1078.

Zhao, X. L., Wang, Y. Y., Wang, Y. R., Liu, Y., and Gao, S., 2017. Histone methyltransferase TXR1 is required for both H3 and H3.3 lysine 27 methylation in the well-known ciliated protist *Tetrahymena thermophila*. *Science China Life Science*, **60**: 264-270.

Zhao, Y., Yi, Z. Z., Warren, A., and Song, W. B., 2018. Species delimitation for the molecular taxonomy and ecology of a widely distributed microbial eukaryotes genus *Euplotes* (Alveolata, Ciliophora). *Proceedings of the Royal Society B: Biological Sciences*, **285**: 20172159.

Zhou, X., Wang, Y., Yun, Y., Xia, Z., Lu, H., Luo, J., and Liang, Y., 2016. A potential tool for diagnosis of male infertility: Plasma metabolomics based on GC-MS. *Talanta*, **147**: 82-89.

(Edited by Qiu Yantao)